

## **A FRACTAL STUDY OF THE SIZE EFFECT OF CONCRETE FRACTURE ENERGY**

N.-Q. Feng, X.-H. Ji, Q.-F. Zhuang, and J.-T. Ding  
Department of Civil Engineering, Tsinghua University, Beijing, P.R. China

### **Abstract**

The three-dimensional crack structure of concrete, which is divergent, discontinuous and complex, is quantitatively described with fractal theory, and the calculation formula of total crack surface area deduced. In accordance with the definition of fracture energy by TC50-FMC, a relation is built between fracture energy and the parameters of micro crack structure in micro crack zone, and hence the size effect problem of fracture energy solved theoretically. The relation was also proved by experiments. Results show that: concrete strength increases with the increase of fracture surface energy  $\gamma_s$ ; concrete strength increases and the significance of the size effect of fracture energy  $G_f$  decreases with the decrease of the structure parameter  $D_c$  of the micro crack zone; the structure of the micro crack zone changes with varying specimen size, so does the value of  $D_c$ ; thickness of specimen also causes the size effect of  $G_f$ .

# 1 Theoretical proof

## 1.1 Relation between fracture energy and ligament height

The different fracture toughness of various part of concrete is caused by large amount of discontinuous pores and micro cracks widely and randomly dispersed, as well as heterogeneity of internal structure of the material. Stress intensity factors of different parts also vary even under the same applied force. The part with lower fracture toughness or higher stress intensity factor always begins to crack first. Therefore, micro cracks caused by external force are also discontinuous and randomly distributed. Like the main macro crack, micro cracks are extremely tortuous and branching. Such a complex and irregular micro crack system can be simulated with a fractal model.

Suppose the micro crack dispersion in micro crack zone is a dendritic structure as shown in Fig. 1a, and assume the length of each broken line segment of the generator (Fig. 1b) to be a unit length, then, according to the following formula:

$$D = \lg N / \lg(1/r),$$

the fractal dimension of crack structure can be calculated with:

$$D = \lg 3 / \lg(2 \cos(\beta/4)).$$

Therefore the fractal dimension of micro crack structure is greater than 1. Though the real micro crack structure is much more complex than the dendritic structure model, it can be qualitatively described with such a model.

Fig. 2 shows the fracture process of the micro and macro cracks of several groups of specimens with different height of ligament. When external force  $P_h$  rises to a certain degree, micro crack zone begins to converge and link up, leading to the starting of fracture, and from then on

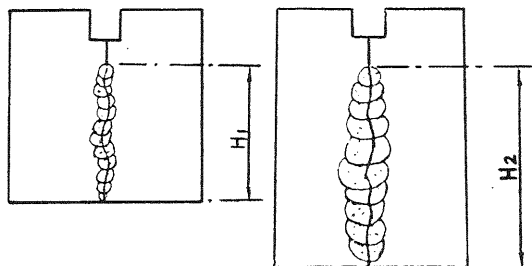
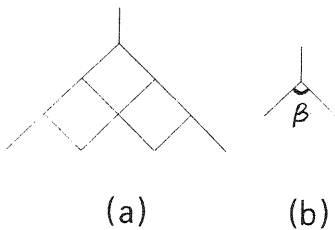


Fig. 1 Dendritic structure of micro cracks in micro crack zone

Fig. 2 Sketch map of micro and main cracking in specimens with different ligament height

the sub-critical propagation process of fracture begins. If the main crack has developed to a certain level, it will turn into a destabilizing propagation. During the whole fracture process (starting of fracture, sub-critical propagation and destabilizing propagation), the micro crack zone always exists at the tip of the crack as a forerunner. Fractal theory is used next to reinvestigate the nonlinear difference of the real fracture surface area caused by the micro crack zone in the specimens of different height shown in Fig. 2.

If a series of dishes are used to cover the fracture surface which corresponds to the fractal structure, the relation among the necessary number of dishes( $N(r)$ ), the radius of the dishes( $r$ ) and the fractal dimension of fracture surface( $D$ ) can be expressed as:

$$N(r) = C r^{-D} \quad (1)$$

where  $C$  is a constant.

If a dish with a constant radius  $r_0$  is used to cover a set of fracture surfaces with various lengths  $R$ , what about the relation between  $N$  and  $R$ ? No matter how irregular a section is, it can be regarded as a part of spherical surface with a radius of  $R_0$  if the magnification times at observing are low enough. When the measuring yardstick, e.g. the radius of the dish, is replaced by  $r$ , the corresponding radius  $r$  is:

$$R = R_0 r_0 / r,$$

$$\text{then } r = R_0 r_0 / R,$$

and the relation between  $N$  and  $R$  can be expressed as:

$$N = C(R_0 r_0)^{-D} R^D = C' R^D, \quad (2)$$

where  $C'$  is also a constant, which equals to  $C(R_0 r_0)^{-D}$ . If  $R = R_0$  and  $r = r_0$ , then Eq. (2) is equated to Eq. (1).

Similarly, if a constant yardstick  $r_0$  is used to measure the fracture surface of specimens (Fig. 2) along the track of the crack in crack expanding direction, the number  $N$  is:

$$N = C' H^{D_c},$$

where the fractal dimension  $D_c$  is not of the macro fracture surface, but of the total crack structure formed during the whole fracture process.

In order to calculate exactly the real length ( $H_r$ ) of the fracture surface

from the height of ligament  $H$ , the least yardstick  $r_0$  should be used which equals to  $2b$  (Hornbogen, 1989). Here  $2b$  represents twice of the atomic space length.

$$H_r = N r_0 = C' r_0 H^{D_c} = C'' H^{D_c},$$

where  $C''=C'r_0=2C'b$ . Then  $A_r$ , the real area of fracture surface, can be calculated from the obtained  $H_r$  :

$$A_r = BH_r = C'' H^{D_c} B,$$

where  $B$  is the thickness of specimen.

Assume the surface energy of concrete to be  $\gamma_s$ , then the total energy  $W$  consumed during the whole fracture process can be expressed as follows:

$$W = 2\gamma_s A_r = 2C'' H^{D_c} B \gamma_s.$$

According to the definition of  $A$  (area of fracture section) and  $G_f$  (fracture energy) by TC50-FMC, then:

$$A = BH$$

$$G_f = W/A = 2\gamma_s C'' H^{D_c-1} \quad (3)$$

It can be seen from Eq. (3) that  $G_f$  is influenced by the following factors:

1. Surface energy of concrete  $\gamma_s$ : fracture energy increases with the increase of surface energy.
2. Fractal dimension  $D_c$  of concrete micro crack zone:  $G_f$  increases as  $D_c$  increases. The value of  $D_c$  is related to the size of the micro crack zone, the density and tortuosity of cracks, the size and shape of specimen and the pattern of loading.
3. Ligament height  $H$  of specimen:  $G_f$  will be greater if  $H$  is higher, but the relation between them is not linear.
4.  $C''$ : It is a factor relating to the least yardstick used to measure the area of fracture surface. The calculated value of  $G_f$  is a function of the least yardstick.

## 1.2 Size effect of $G_f$

The relation between  $G_f$  and  $H$ , as shown in Eq. (3), indicates the size effect of  $G_f$ . It can be changed into a differential form:

$$\frac{dG_f}{dH} = 2\gamma_s c'' (D_c - 1) H^{D_c} / H^2 \quad (4)$$

If the material is an ideal elastic and brittle body, the fracture surface would be a plane, that is,  $D_c=1$  and  $dG_f/dH=0$ . It means that  $G_f$  of such a material does not relate to  $H$  and has no size effect. But in cement-based materials there is always a micro crack zone at the tip of the main crack. Therefore,  $1 < D_c < 2$  and  $dG_f/dH > 0$ , showing that  $G_f$  is an increasing function of  $H$ .  $D_c$  increases with the size of micro crack zone, the density and tortuosity of micro cracks in the zone. This will lead to a more significant size effect.

If  $D_c$  is of a great value,  $H^{D_c}/H^2$  would be very small because  $1 < D_c < 2$ , so that  $dG_f/dH$  would be small too. It means that if the size of specimen is great enough, the size effect of  $G_f$  can be ignored.

From Eq. (3) the size effect caused by the thickness  $B$  of specimen can also be deduced. The relation between  $B$  and  $G_f$  is similar to that of  $H$  and  $G_f$ .

$D_c$  can be regarded as an index of the significance of the size effect of  $G_f$ . If  $D_c$  is known,  $G_f$  can be well calculated.

### 1.3 Fractal dimension $D_c$ of micro crack structure

The logarithmic form of Eq. (3) is

$$\lg G_f = \lg(2\gamma_s C'') + (D_c - 1) \lg H \quad (5)$$

so  $D_c-1$  can be obtained by regressing in  $\lg G_f$ - $\lg H$  coordinate and  $D_c$  got. The intercept  $S$  of straight line can be expressed as:

$$S = (G_f)_{H=0} = \lg(2\gamma_s C'') \quad (6)$$

Since  $C''$  is a constant,  $\gamma_s$  can be evaluated if  $S$  has been obtained. The higher the intercept is, the greater the surface energy. Wittmann (1991) has recommended a method to calculate the surface energy of concrete material by expolation:

$$\gamma_s = g(a)_{H=0} \quad (7)$$

in which  $g(a)$  is a distribution function of  $G_f$  along the whole height of fracture ligament. It can be seen that the methods to evaluate  $\gamma_s$  by Eq. (6) and Eq. (7) are similar.

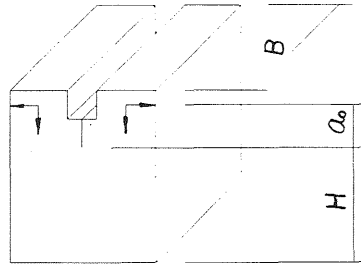


Fig. 3 Sketch map of specimen parameters

## 2 Experimental test

### 2.1 Size effect according to the height $H$ of ligament

#### 2.1.1 Specimens and concrete mixture

Fig. 3 shows the geometric parameters and loading pattern of the fracture specimen. Concrete mix proportions are listed in Table 1.

Table 1. Mix proportion and compressive strength of concrete

No.	Materials ( $\text{kg}/\text{m}^3$ )							28d Compressive strength (MPa)
	W/C	Enhancer	Cement	Water	Sand	Gravel	NF*	
1	0.45	----	450	203	575	1222	----	44.9
2	0.30	----	550	165	541	1264	55	66.8
3	0.30	55	495	165	541	1264	55	74.4

\*NF is a brand of superplasticizer.

#### 2.1.2 Obtainment of different height of ligament

Two methods were used to obtain different  $H$ :

1. With a constant  $W(W=H+a_0)$  of 18.45 cm, original crack length  $a_0$  was set at the value of 3.95 cm, 6.65 cm, 8.45 cm, and 10.3 cm for each group of specimens, and the corresponding  $H$  was 14.5 cm, 11.8 cm, 10.0 cm and 8.15 cm respectively. The concrete mixture is as No. 2 in Table 1.
2. With a constant  $a_0$  of 3.95 cm,  $H$  was set at the value of 14.55 cm, 12 cm, 10.0 cm, 8.0 cm, 6.0 cm and 4.0 cm. The concrete mixtures are listed in Table 1. as No. 1, 2 and 3.

## 2.2 Experimental determination

P-COD curves at different H are shown in Fig. 4. Fig. 5 shows the  $G_f$ -H relation regressed in  $\lg G_f$ - $\lg H$  coordinate. Some parameters of the two kinds of specimens with different H are listed in Table 2, where K is the slope, S the intercept, r the correlation coefficient, and  $D_c$  the fractal dimension.

Table 2. Parameters of two kinds of specimens with different H

Type of specimens	K	S	r	$D_c$
1. set W, change $a_0$	0.4406	1.9534	0.9787	1.4406
2. set $a_0$ , change W	0.4950	1.9089	0.9950	1.4950

In Table 2,  $D_c$  of Type 1 is smaller than that of Type 2. It indicates that the size effect of  $G_f$  of the latter is much larger. The parameters listed in Table 2 also show that the size effect relates significantly to the shape of specimens.

## 2.3 Size effect of $G_f$ of Type 2

Concrete mixtures are listed in Table 1 as No. 1, 2 and 3. The relation between fracture toughness  $K_{IC}$  of the concrete with different W/C and height of ligament H is shown in Fig. 6, indicating that the lower the W/C, the greater the compressive strength and  $K_{IC}$  of concrete. With the same W/C, the concrete with strength enhancer has higher compressive strength and fracture toughness  $K_{IC}$ . Fig. 7 shows the regressed relation between

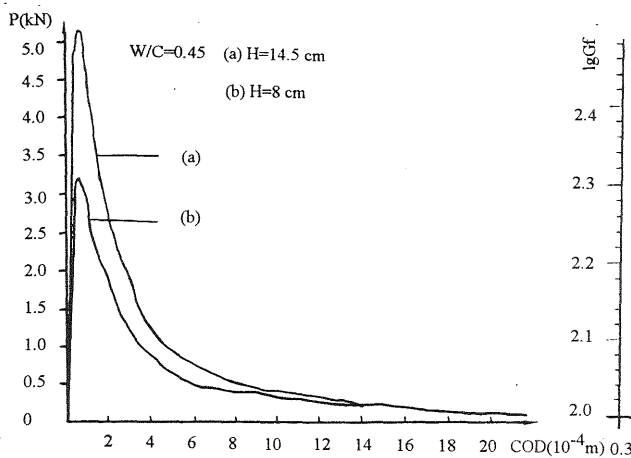


Fig. 4 P-COD curves at different H

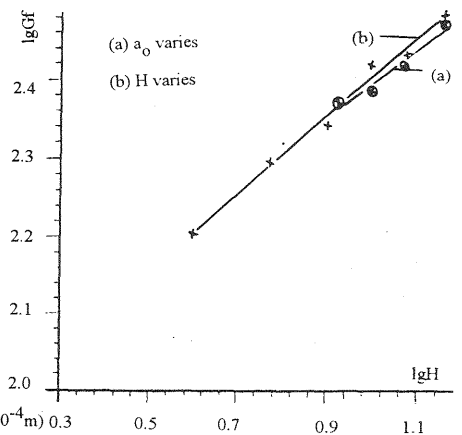


Fig. 5  $\lg G_f$  versus  $\lg H$  of concrete with different shapes

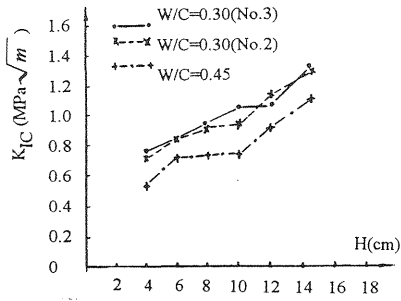


Fig. 6  $K_{IC}$  of concretes with different W/C and ligament height H

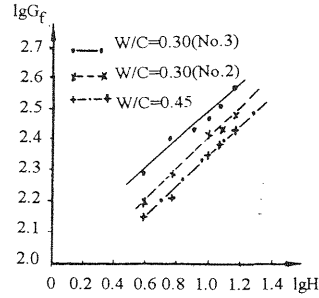


Fig. 7 Regressed  $\lg G_f$ - $\lg H$  of three kinds of concrete

$\lg G_f$  and  $\lg H$  of three kinds of concrete. The parameters such as K (slope), S (intercept), r (correlation coefficient) and  $D_c$  (fractal dimension) of the three straight lines in Fig. 7 are listed in Table 3.

Table 3. Parameters of concrete with different W/C

W/C	Type of concrete	K	S	r	$D_c$
0.3	reference concrete	0.495	1.9089	0.995	1.495
0.3	concrete with enhancer	0.4532	2.031	0.993	1.4532
0.45	reference concrete	0.5039	1.855	0.984	1.5039

Table 3 shows that if the concrete compressive strength increases, the value of  $D_c$  decreases. It also indicates that the strength enhancer causes induction of  $D_c$ . Surface energy  $\gamma_s$  is raised with improvement of concrete compressive strength.  $D_c$  shows the influence of micro crack zone upon the deterioration of concrete. The greater the  $D_c$ , the greater the density and tortuosity of micro crack zone and the more damage of the concrete structure during the whole fracture process.

#### 2.4 Influence of B upon $G_f$

The concrete mix proportion is listed in Table 1 as No. 1. The thicknesses B of specimens were set at the value of 4.5 cm, 7.2 cm, 10.0 cm and 20.0 cm, and the other size parameters were set as follows:  $a_0=3.95$  cm,  $W=18.45$  cm,  $H=14.5$  cm. The relation between  $K_{IC}$  and B is shown in Fig. 8, CTOD<sub>c</sub> (critical crack tip opening displacement) and B in Fig. 9,  $G_f$  and B in Fig. 10, and a corresponding regression line obtained in  $\lg G_f$ - $\lg B$  coordinate in Fig. 11.

The following conclusions can be drawn from Figs. 8~11:



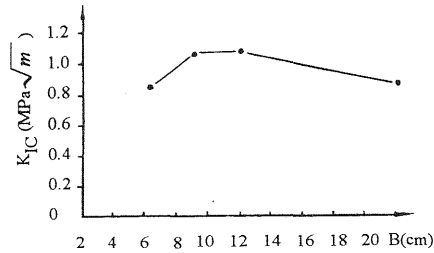


Fig. 8  $K_{IC}$  versus B of concrete

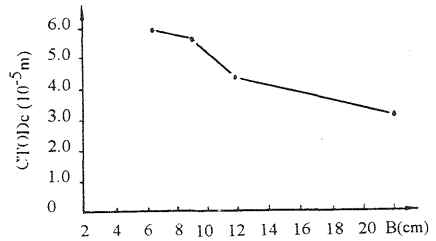


Fig. 9  $CTOD_c$  versus B of concrete

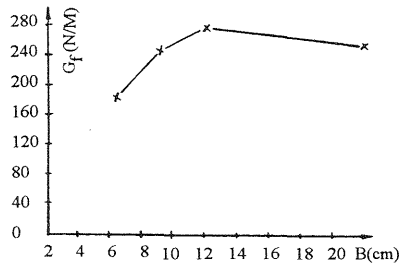


Fig. 10  $G_f$  versus B of concrete

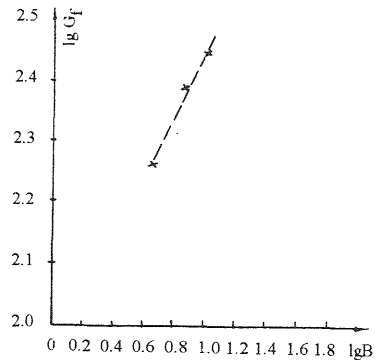


Fig. 11 Regressed  $lg G_f$ - $lg B$  of concrete

1. The influence of B on  $K_{IC}$  is not marked.  $K_{IC}$  increases with B at first, but when B is larger than a certain level,  $K_{IC}$ -B curve goes down.
2. The value of  $CTOD_c$  decreases as B increases. The increasing of B leads to greater brittleness of concrete and smaller value of  $CTOD_c$  when the crack is in a destabilized propagation.
3. The relationship between  $G_f$  and B is similar with the one between  $K_{IC}$  and B. But if  $B > 10$  cm,  $G_f$  increases with the increase of B. When the thickness of specimen is larger than a certain value, the rupture of concrete is more like the plain strain fracture, and leads to low values of  $G_f$  and  $K_{IC}$ .
4. In Fig. 9, the points at  $B=4.5$  cm, 7.2 cm and 10.0 cm, are regressed to be a straight line with  $r=0.993$ ,  $S=1.918$  and  $D_c=1.536$ . But the point at  $B=20$  cm is far away from the regression line. It proves that only when B is in a certain range, is Eq. (3) an effective expression for the plain stress fracture of concrete.

### 3 Conclusions

The basic reason for the size effect of  $G_f$  is that there is always a micro crack zone at the tip of the main macro crack during the whole fracture process. At present, the definition of the area of fracture surface by TC50-FMC is obviously too small. The fracture surface area should include the area of the total crack surface produced during the whole fracture process, especially the area of the great amount of micro cracks. The structure of the micro crack zone should include the size of micro crack zone, the density and tortuosity of micro cracks.

With fractal theory, the structure of micro crack zone is simplified to a dendritic structure, and its fractal dimension obtained.

In this paper, the most essential formulae of fractal theory were studied from another angle. According to the definition of  $G_f$  by TC50-FMC, a formula was deduced to express the relation between  $G_f$  and  $H$ ,  $\gamma_s$  and  $D_c$  (see Eq. (3)). Theoretical analysis showed that  $G_f$  is an increasing function of  $\gamma_s$ ,  $H$  and  $D_c$ . If the value of  $H$  is large enough, the size effect of  $G_f$  can be ignored.

The formula which describes the relation between  $G_f$  and the geometry parameters was also proved by experiment. The results show that:

1. The surface energy  $\gamma_s$  increases with concrete strength;
2. With the improvement of concrete strength, the structure parameter  $D_c$  in the micro crack zone decreases, and so does the magnitude of the size effect of  $G_f$ ;
3. When the size of the specimen varies, the structure of the micro crack zone changes, and so does the value of  $D_c$ ;
4. The thickness of the specimen also causes size effect of  $G_f$ .

### 4 References

- Hornbogen, E. (1989) Fractals in microstructure of metals. **International Materials Reviews**, 6, 277-296.
- RILEM Draft Recommendation (1985) Determination of the fracture energy of mortar and concrete by means of three-point-bend tests on notched beams. **Materials & Structures**, 106, 286-290.
- Wittmann, F.H. et al. (1991) Fracture process zone in cementitious materials. **International Journal of Fracture**, 1, 3-18.